

# SUPER EFFICIENT GEODESICS IN THE COMPLEX OF CURVES

XIFENG JIN AND WILLIAM MENASCO

ABSTRACT. We introduce a subclass of efficient geodesics, called *super efficient geodesics*, that the bound of intersection number in initial efficiency only depends on the genus of surface. For any two vertices,  $v, w \in \mathcal{C}(S_g)$ , in the complex of curves of a closed oriented surface of genus  $g \geq 2$ , and any efficient geodesic,  $v = v_1, \dots, v_d = w$ , it was previously established by Birman, Margalit and the second author [4] that there is an explicitly computable list of at most  $d^{(6g-6)}$  candidates for the  $v_1$  vertex. In this note we establish a bound for this computable list for super efficient geodesics that is independent of  $d$ -distance and only dependent on genus. The proof relies on an intersection growth inequality (IGI) between intersection number of two curves and their distance in the complex of curves, together with a thorough analysis of the dot graph associated with the intersection sequence.

## 1. INTRODUCTION

Let  $S = S_g$  be a closed oriented surface of genus  $g \geq 2$ . The *complex of curves* or *curve complex* of surface  $S$  is a simplicial complex such that each vertex corresponds to the isotopy class of an essential simple closed curve, and  $n + 1$  vertices form an  $n$ -simplex of  $\mathcal{C}(S)$  if their representatives can be realized disjointly. At times we will use the words “vertices” and “curves” interchangeably, and use curve as essential simple closed curve. For any two curves  $v$  and  $w$  in  $\mathcal{C}(S)$ , the *distance*  $d(v, w)$  is the minimal number of edges in  $\mathcal{C}(S)$  connecting  $v$  to  $w$ . A *geodesic* in  $\mathcal{C}(S)$  is a sequence of vertices  $\Gamma = (\gamma_i)_{i \in I}$  such that  $d(\gamma_i, \gamma_j) = |i - j|$  for all  $i, j \in I$ .

Harvey [8] introduced the curve complex in 1978 as a tool for studying the mapping class group of a surface. In 1996, Masur and Minsky [11] proved the seminal result that  $\mathcal{C}(S)$  is  $\delta$ -hyperbolic. However, the computation of distance in  $\mathcal{C}(S)$  is still very intimidating. The first attempt of such algorithm was due to Leasure [10] in his thesis in 2002. After that, there are several other algorithms found by Shackleton [13], Webb [15], and Watanabe [14], in which all algorithms utilize the notion of *tight geodesics* that were first constructed in a sequel [12] of Masur-Minsky’s work [11]. In an initial paper by Birman, Margalit, and Menasco [4], efficient geodesics were introduced as an alternative preferred set of geodesics to compute the distance in  $\mathcal{C}(S)$ .

Suppose  $v_0, v_1, \dots, v_d$  is a geodesic of length  $d \geq 3$  in  $\mathcal{C}(S)$ , and  $\alpha_0, \alpha_1, \alpha_d$  are representatives of  $v_0, v_1, v_d$  that are pairwise in minimal position. A *reference arc* for  $\alpha_0, \alpha_1, \alpha_d$  is an arc  $\gamma$  that is in minimal position with  $\alpha_1$  and whose interior is disjoint from  $\alpha_0 \cup \alpha_d$ . The geodesic  $v_0, v_1, \dots, v_d$  is *initially efficient* if  $|\alpha_1 \cap \gamma| \leq d - 1$  for all possible reference arcs. Moreover, the geodesic is called *efficient*, if the oriented

---

*Date:* 10:32 Sunday 22<sup>nd</sup> December, 2024.

*2010 Mathematics Subject Classification.* Primary: 57M60. Secondary: 20F38.

*Key words and phrases.* complex of curves, efficient geodesics, intersection growth inequality, super efficient geodesics, super efficiency.

geodesic  $v_k, v_{k+1}, \dots, v_d$  is initially efficient for  $0 \leq k \leq d - 3$  and the oriented geodesic  $v_d, v_{d-1}, v_{d-2}, v_{d-3}$  is also initially efficient. The *complexity of a path*  $v = v_0, v_1, \dots, v_n = w$  in  $\mathcal{C}(S)$  is defined to be  $\sum_{k=1}^{n-1} (i(v_0, v_k) + i(v_k, v_n))$ . The existence of initially efficient geodesics was justified by the geodesics  $v = v_0, v_1, \dots, v_d = w$  of minimal complexity. For more details about efficient geodesics, we refer the readers to the paper [4], where the main result is that such efficient geodesics always exist, and there are only finitely many between any two vertices. Specifically, in [4] it is established that there is an explicitly computable list of at most

$$d^{6g-6}$$

vertices,  $v_1$ , that can appear as the first vertex of an (initially) efficient geodesic  $v = v_0, v_1, \dots, v_d = w$ .

Our key advancement for this note is the establishment of a subclass of efficient geodesics, called *super efficient geodesics*, that the bound of intersection number with reference arcs is  $\min(d - 1, 15 \cdot (6g - 8))$  for genus  $g \geq 3$  and  $\min(d - 1, 44)$  for  $g = 2$ . This property of a geodesic is called *super efficiency*. In [4], it was argued that any geodesic could be replaced by an initially efficient geodesic; that is,  $|\alpha_1 \cap \gamma| \leq d - 1$ , for all possible reference arcs  $\gamma$ . The existence of super efficient geodesics will follow from altering this distance-dependent intersection bound to one that is dependent on genus.

**Theorem 1.1.** *Let  $v$  and  $w$  be two curves on a closed oriented surface  $S_{g \geq 2}$  with distance  $d(v, w) \geq 3$ , then there exists a super efficient geodesic  $v = v_0, v_1, \dots, v_d = w$  in  $\mathcal{C}(S_g)$ . More precisely, suppose  $\alpha_0, \alpha_1$  and  $\alpha_d$  are minimal intersecting representing curves of  $v_0, v_1$  and  $v_d$ , respectively. Let  $\gamma$  be any reference arc for the pair  $(\alpha_0, \alpha_d)$ . Then for  $g = 2$ , we have  $|\alpha_1 \cap \gamma| \leq \min(d - 1, 44)$ ; and for  $g \geq 3$ , we have  $|\alpha_1 \cap \gamma| \leq \min(d - 1, 15 \cdot (6g - 8))$ .*

Similar to the efficient geodesics, the existence of super efficient geodesics will be justified by the geodesics of minimal total complexity. Among the geodesics between the two curves, the relationship between these three categories is as follows,

$$\{\text{geodesics of minimal total complexity}\} \subset \{\text{super EG}\} \subset \{\text{EG}\},$$

where EG stands for efficient geodesics.

As a result, we obtain a new bound on the size of this explicit list of the candidates for  $v_1$  vertex in the super efficient geodesics that is independent of distance and only dependent on genus. In particular, we have the following corollary.

**Corollary 1.2** (Super efficiency). *If  $v = v_0, v_1, \dots, v_d = w$  is a super efficient geodesic of  $\mathcal{C}(S_g)$  with  $d(v, w) = d \geq 3$ , then, for  $g > 2$ , there is an explicitly computable list of at most*

$$[15 \cdot (6g - 8) + 1]^{6g-6}$$

vertices  $v_1$  that can appear as the first vertex on an (initially) super efficient geodesic. When  $g = 2$  the bound on this list is  $45^6$ .

It is useful to extend the discussion begun in the introduction of [4] comparing the bounds on the size of the set of  $v_1$  candidates given by the use of super efficient geodesics and the bounds by the use of tight geodesics. From that discussion we have the bound results coming from the work of Webb [15] which gives a bound of  $2^{(72g+12)\min\{d-2,21\}}(2^{6g-6} - 1)$ . In particular, when  $d - 2 \geq 21$  and  $g = 2$  we get a bound that is  $\sim 10^{75}$ . Whereas, a super efficiency bound for  $g = 2$  is  $\sim 10^{10}$  and independent of distance.

Additionally, some discussion is warranted for how efficient geodesics and super efficient geodesics might be utilized in constructing an algorithm for computing distance in the curve complex. In [3] Bell and Webb describe a polynomial time algorithm based on the Masur-Minsky's tight geodesics technology for computing distance in the curve complex. A key feature of their description is the "train-track-type" behavior of curves representing the vertices of a tight geodesic. A distance algorithm utilizing super efficient geodesics will exhibit similar behavior. Specifically, the  $6g - 6$  exponent in the Corollary 1.2 bound comes from the dimension of the Dehn-Thurston coordinate space for simple closed curves on  $S_g$ . A particular  $\gamma$ -coordinate of an  $\alpha$  curve corresponds to the intersection number with a specified  $\gamma$ -curve or, in a surface with boundary which is the setting for efficient geodesic technology, an  $\gamma$ -arc. Having the bound coming from Theorem 1.1 means any  $\gamma$ -coordinate of an  $\alpha_1$  can only assume a value between 0 and  $15 \cdot (6g - 8)$ . Super efficiency of the geodesic then forces the  $\gamma$ -coordinate of  $\alpha_2$  to be greater than or equal to  $|\alpha_1 \cap \gamma| - 1$  but still bounded by  $\min\{d - 2, [15 \cdot (6g - 8)]\}$ . In general, for the  $\gamma$ -coordinate of  $\alpha_{i+1}$ , we will have  $|\alpha_i \cap \gamma| - 1 \leq |\alpha_{i+1} \cap \gamma| \leq \min\{d - (i + 1), [15 \cdot (6g - 8)]\}$ ,  $1 \leq i \leq d - 3$ . Thus, the  $\gamma$ -coordinates of smaller indices  $\alpha$ 's are restricting the behavior of larger indices  $\alpha$ 's. It is then reasonable to think that an efficient geodesic based algorithm would be of polynomial time.

Recall for two curves,  $\alpha, \beta \subset S_g$ , their *intersection number*,  $|\alpha \cap \beta|$ , is the minimal possible number of intersections between  $\alpha$  and  $\beta'$  where  $\beta'$  is any curve isotopic to  $\beta$ . A *filling pair* of curves is a pair of curves,  $(\alpha, \beta)$  with  $d(\alpha, \beta) \geq 3$ . In other words, the complement of  $\alpha \cup \beta$  in the surface  $S_g$  is a union of discs. To prove Theorem 1.1, we need a tight bound for the distance between any two vertices in terms of their intersection number, which is called the *intersection growth inequality* or *IGI*.

**Theorem 1.3** (The IGI). *Let two curves  $\alpha, \beta \subset S_g$  represent two vertices  $v, w \in \mathcal{C}(S_g)$  that realize their intersection number. If  $g = 2$  and  $d(v, w) = d \geq 4$  then*

$$2^{d-4} \cdot 12 \leq |\alpha \cap \beta|.$$

*If  $g > 2$  and  $d(v, w) = d \geq 3$  then*

$$2^{d-3} \cdot (2g - 1) \leq |\alpha \cap \beta|,$$

that is,

$$d \leq 2 + \log_2 \left( \frac{|\alpha \cap \beta|}{g - 0.5} \right).$$

The IGI takes into account of the genus of surface, so it is slightly better than the following estimate given by Hempel [9]:

$$(1) \quad d(\alpha, \beta) \leq 2 + 2 \cdot \log_2(|\alpha \cap \beta|)$$

Another estimate utilizes the topology of a surface was proved by Bowditch (Corollary 2.2 in [5]) and reformulated by Aougab, Patel and Taylor [2].

**Theorem 1.4.** *For any two curves  $\alpha$  and  $\beta$  on an oriented surface  $S_{g,p}$  with Euler characteristic  $|\chi(S_{g,p})| \geq 5$  and  $|\alpha \cap \beta| > 0$ ,*

$$(2) \quad d(\alpha, \beta) < 2 + 2 \cdot \frac{\log_2(|\alpha \cap \beta|/2)}{\log_2((|\chi(S_{g,p})| - 2)/2)}.$$

From the asymptotic perspective, a much stronger result was provided by Aougab (Theorem 1.2 in [1]) to show the uniform hyperbolicity of curve graphs.

**Theorem 1.5.** *For each  $\lambda \in (0, 1)$ , there is some  $N = N(\lambda) \in \mathbb{N}$  such that if  $\alpha, \beta \in \mathcal{C}_0(S_{g,p})$ , whenever  $\xi(S_{g,p}) > N$  and  $d_C(\alpha, \beta) \geq k$ ,*

$$(3) \quad |\alpha \cap \beta| \geq \left( \frac{\xi(S_{g,p})^\lambda}{f(\xi(S_{g,p}))} \right)^{k-2},$$

where  $f(\xi) = O(\log_2(\xi))$ .

**Remark 1.6.** *For a closed oriented surface  $S_{g \geq 4}$ , Bowditch's estimate becomes*

$$d(\alpha, \beta) < 2 + 2 \cdot \frac{\log_2(|\alpha \cap \beta|/2)}{\log_2(g - 2)}.$$

*If  $2 \leq g \leq 6$ , then the upper bound on the right of the last inequality in the IGI is smaller. Otherwise, Bowditch's estimate is smaller as long as the intersection number of two curves is sufficiently large. The bound in Theorem 1.1 is obtained with the IGI.*

The paper is organized as follows. In section 2, we utilize the intersection number of a minimal filling pair as a lower bound and linear integer programming to establish the growth rate to prove Theorem 1.3. In section 3, we review the techniques of efficient geodesics from [4] that we will use in later sections. In section 4, we use the one-vertex triangulation of surface to show that some parallel arcs occur as the intersection number is sufficiently large, and we call such parallel arcs a *rainbow*. In the last section 5, we investigate the pattern hidden in the dot graph that arises as a rainbow and complete the proof of Theorem 1.1. Super efficiency of Corollary 1.2 follows.

## ACKNOWLEDGEMENT

The second author wishes to thank Dan Margalit for numerous conversations he had with him during the development of this project. Similarly, the second author thanks Joan Birman for numerous discussions on the curve complex and efficient geodesics. We also wish to thank Kasra Rafi for alerting us to Brian Bowditch's growth rate result in [5], and thank Tarik Aougab for letting us know his asymptotic growth rate in Theorem 1.5 in [1]. Finally, we would like to thank an anonymous reviewer for pointing out an error in our original statement of Theorem 1.1 and many other helpful comments that improved the exposition.

## 2. ESTABLISHING THE IGI

The proof of Theorem 1.1 will need to use the behavior of efficient geodesics and an estimate on the growth rate of the intersection number of filling pairs of curves with respect to distance. Specifically, we first will give a proof of the IGI.

*Proof of Theorem 1.3.* The idea of our proof for establishing these growth inequalities is to utilize the *linear integer program* (LIP) approach that was developed in the work of Glenn, Morrel, Morris and the second author [7] to establish the following result.

**Theorem 2.1.** *The minimal intersection number for a filling pair,  $\alpha, \beta \subset S_2$ , representing vertices  $v, w \in \mathcal{C}(S_2)$ , respectively, with  $d(v, w) = 4$  is 12.*

First, let us recall the LIP argument. Suppose that  $(\alpha, \beta)$  is a filling pair for  $S_2$ , and we split  $S_2$  along  $\alpha$  and consider the resulting properly embedded arcs of  $\beta$  in a genus one surface having two boundary components,  $S_{1,2}$ . (As in [4], we can reduce to the case where  $\alpha$  is non-separating so that the surface is connected.) Assume that  $\alpha$  and  $\beta$  are arranged to be minimally intersecting up to isotopy, we can assume that all the discs of  $S_{1,2} \setminus \beta$  are  $2k$ -gons,  $k \geq 2$ . Now consider an essential curve,  $c \subset S_{1,2}$ , that intersects each arc of  $\beta$  at most once. We notice that  $|c \cap \beta|$  has to be sufficient so that  $d(c, \beta) \geq d(\alpha, \beta) - 1$ . In particular, if  $d(\alpha, \beta) = 4$ , we have to have  $|c \cap \beta| \geq 4$ , since 4 is the minimal intersection number for the pair  $(c, \beta)$  to be filling.

We can translate this above discussion into a system of linear inequalities, one for each such simple closed curve  $c$ . First, in  $S_{1,2}$  we can collapse all bands of 4-gon regions to a single properly embedded arc. This gives us a collection of non-parallel properly embedded essential arcs in  $S_{1,2}$ . If need be we throw in additional essential arcs such that our collection,  $C$ , is a maximal collection of non-parallel properly embedded essential arcs in  $S_{1,2}$ . Such a maximal collection splits  $S_{1,2}$  up into four 6-gon disc regions. (Up to homeomorphism there are only a finite number of ways gluing together four 6-gons to construct  $S_{1,2}$ .) The left illustration in Figure 1 shows

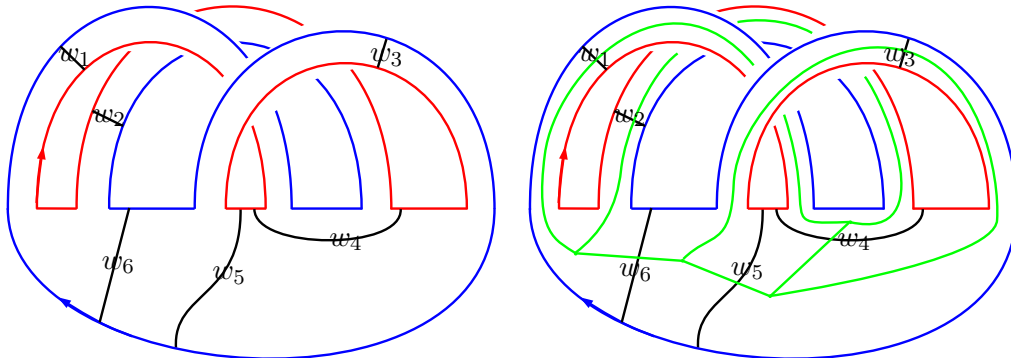


FIGURE 1. The left illustration is a genus one surface with two boundary curves—coded red and blue.  $C$  is a maximal collection of 6 weighted arcs. The weights,  $w_1, w_2, w_3, w_4, w_5, w_6$ , are non-negative integers. In Theorem 2.1, all weights can be taken to be equal to 2 for  $\beta$ . The green graph in the right illustration is  $G(C)$ , the dual graph. Each edge of  $G(C)$  intersects exactly one arc of  $C$  once.

one possible 6-gon decomposition of  $S_{1,2}$ . To find all possible loops,  $c$ , of the required type that intersect any essential arc in our collection at most once, we consider the dual graph,  $G(C)$ , to this decomposition, as illustrated in the right of Figure 1. One of our needed curves is then just a circuit—a closed edge-path—in  $G(C)$ . To each such circuit we associate an inequality as follows.

First, assign weights,  $w_1, w_2, w_3, w_4, w_5, w_6$ , to each of the six essential arcs in the decomposition. Each  $w_i$  corresponds to the number of parallel arcs of  $\beta$ . Next, for any circuit add together all the weights of the arcs of  $C$  that the circuit intersects. For a circuit  $c \subset G(C)$ , this sum is equal to  $|c \cap \beta|$ . Thus, by our previous discussion this sum is greater than 4 when  $d(\alpha, \beta) = 4$ . The circuits of Figure 1 yield the following LIP system (4).

$$\begin{aligned}
 & w_1 + w_4 + w_5 + w_6 \geq 4 \\
 & w_2 + w_4 + w_5 + w_6 \geq 4 \\
 & \phantom{w_2 + w_4 +} w_3 + w_5 \geq 4 \\
 & \phantom{w_2 + w_4 +} w_1 + w_2 \geq 4 \\
 & w_1 + w_3 + w_4 + w_6 \geq 4 \\
 & w_2 + w_3 + w_4 + w_6 \geq 4 \\
 & w_1, w_2, w_3, w_4, w_5, w_6 \geq 0
 \end{aligned}
 \tag{4}$$

When we minimize  $P(w_1, \dots, w_6) = \sum w_i$  constrained by LIP (4), we find that the minimum value of  $P$  is 8, which is **twice** 4—the *scaling factor of  $P$  constrained by LIP (4)*. The minimum value of  $P$  is obtained when  $w_1 = w_2 = w_3 = w_5 = 2$

and  $w_4 = w_6 = 0$ . (One can utilize <https://www.easycalculation.com/operations-research/simplex-method-calculator.php> online.)

**Remark 2.2.** *In order to re-glue the two boundary curves of  $S_{1,2}$  so that in  $S_2$  we obtain the curve  $\beta$ , it is necessary that the sum of the weight on each boundary curve to be equal—an added constraint to (4) that is currently missing. With such an added constraint, as noted in [7], any other 6-gon decomposition of  $S_{1,2}$  will produce an LIP that is equivalent to LIP (4) up to relabeling. So the minimization of  $P$  will still result in a value of 8.*

By the linearity of LIP (4), if we replaced every occurrence of the lower bound of 4 by 1 and asked what would the minimal value of  $P$  so constrained, our answer would be 2. Now the minimal intersection for a distance 4 filling pair as stated in Theorem 2.1 is 12, not 8. This value was obtained by doing a search for distance 4 filling pair utilizing the MICC program [6] that is an implementation of the efficient geodesic algorithm and this search was simplified by starting with filling pairs having at least 8 intersections. Knowing this additional fact we can conclude that any distance 5 filling pair of  $S_2$  must have intersection number at least  $2 \times 12$ . And, in general we have our claimed inequality

$$2^{d-4} \cdot 12 \leq |\alpha \cap \beta|$$

for a filling pair of distance  $d$ .

Finally, we consider a filling pair,  $(\alpha, \beta)$  for a higher genus  $S_g$  and we split along  $\alpha$  to produce  $S_{(g-1),2}$ , we observe that there will always be an embedded  $S_{1,2}$  in  $S_{(g-1),2}$ , for  $g \geq 3$ . Thus, when we produce a 6-gon decomposition for  $S_{(g-1),2}$  coming from a complete collection of non-parallel essential properly embedded arcs, the associated LIP for the dual graph will contain (up to relabeling) a copy of LLP (4). It follows that the scaling factor of  $P$ —the sum of all the weights—is at least 2. This observation plus the fact that  $2g - 1$  is the minimal intersection number for a filling pair yields the inequality:

$$2^{d-3} \cdot (2g - 1) \leq |\alpha \cap \beta|.$$

□

### 3. EFFICIENT GEODESICS

In this section, we will recall some fundamentals of efficient geodesics from [4]. Let  $v$  and  $w$  be vertices of  $\mathcal{C}(S_g)$  with  $d(v, w) = d \geq 3$  and  $v = v_0, v_1, \dots, v_d = w$  be a geodesic connecting  $v$  to  $w$ . The intersection between the representatives  $\alpha_i$  of  $v_i$  and the reference arc  $\gamma$  produces a sequence of natural numbers along  $\gamma$ , which is called the *intersection sequence* of the  $\alpha_i$  along  $\gamma$ .

An intersection sequence  $\sigma$  of natural numbers  $(j_1, j_2, \dots, j_k)$  can be arranged in a normal form called *sawtooth form*, that is,

$$j_i \leq j_{i+1} \implies j_{i+1} = j_i + 1.$$

If the intersection sequence in sawtooth form is viewed as a function  $\{1, 2, \dots, N\} \rightarrow \mathbb{N}$ , where  $N$  is the cardinality of  $\gamma \cap (\alpha_1 \cup \alpha_2 \cup \dots \cup \alpha_{d-1})$ , then the graph is a set of lattice points of integer coordinates. The graph of the sequence is called *dots*, and the line segments resulting from the join of dots with slope 1 are called *ascending segments*. The resulting graph of intersection sequence  $\sigma$  in sawtooth form is called the *dot graph*, denoted by  $G(\sigma)$ . An example of dot graph is illustrated in Figure 2.

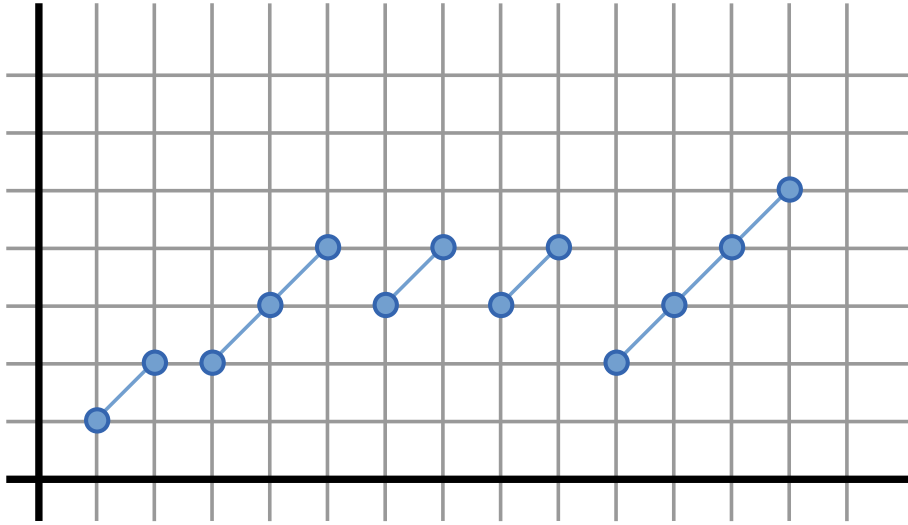


FIGURE 2. A typical dot graph of intersection sequence in sawtooth form.

Next, we will deal with certain shapes of polygons in the dot graph. A polygon in the plane is a *dot graph polygon* if

- (1) the edges all have slope 0 or 1,
- (2) the edges of slope 0 have nonzero length, and
- (3) the vertices all have integer coordinates.

The edges of slope 1 in a dot graph polygon are called *ascending edges* and the edges of slope 0 are called *horizontal edges*.

Let  $\sigma$  be a sequence of natural numbers in sawtooth form. A dot graph polygon is a  $\sigma$ -*polygon* if:

- (1) the vertices are dots of  $G(\sigma)$  and
- (2) the ascending edges are contained in ascending segments of  $G(\sigma)$ .

A *box* in  $G(\sigma)$  is a  $\sigma$ -quadrilateral  $P$  with the following two properties:

- (1) the leftmost ascending edge contains the highest point of some ascending segment of  $G(\sigma)$  and



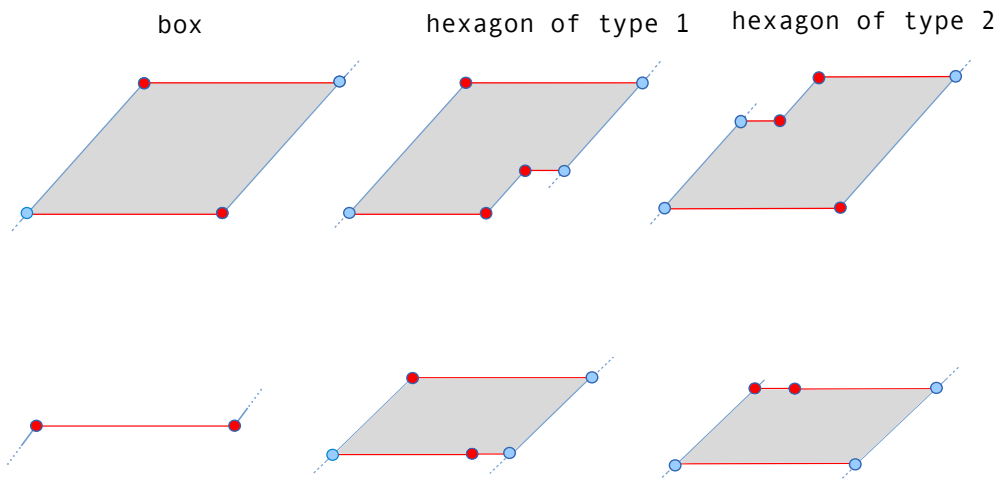


FIGURE 3. Box and hexagons of types 1 and 2 on the top; Corresponding degenerate box and hexagons at the bottom. Red dots are endpoints of ascending segments, and blue dots may or may not be endpoints.

- (2) the rightmost ascending edge contains the lowest point of some ascending segment of  $G(\sigma)$ .

Up to translation and changing the edge lengths, there are four types of dot graph hexagons; two have an acute exterior angle, and we will not need to consider these. Notice that a dot graph hexagon necessarily has a leftmost ascending edge, a rightmost ascending edge, and a middle ascending edge. This holds even for degenerate hexagons since horizontal edges are required to have nonzero length.

A *hexagon of type 1* in  $G(\sigma)$  is a  $\sigma$ -hexagon where:

- (1) no exterior angle is acute,
- (2) the middle ascending edge is an entire ascending segment of  $G(\sigma)$ , and
- (3) the minimum of the middle ascending edge equals the minimum of the leftmost ascending edge,
- (4) the leftmost ascending edge contains the highest point of an ascending segment of  $G(\sigma)$ .

Similarly, a *hexagon of type 2* in  $G(\sigma)$  is a  $\sigma$ -hexagon that satisfies the first two conditions above and the following third and fourth conditions:

- (3') the maximum of the middle ascending edge equals the maximum of the rightmost ascending edge,
- (4') the rightmost ascending edge contains the lowest point of an ascending segment of  $G(\sigma)$ .

See Figure 3 for pictures of boxes and hexagons of types 1 and 2 and their degenerate cases.

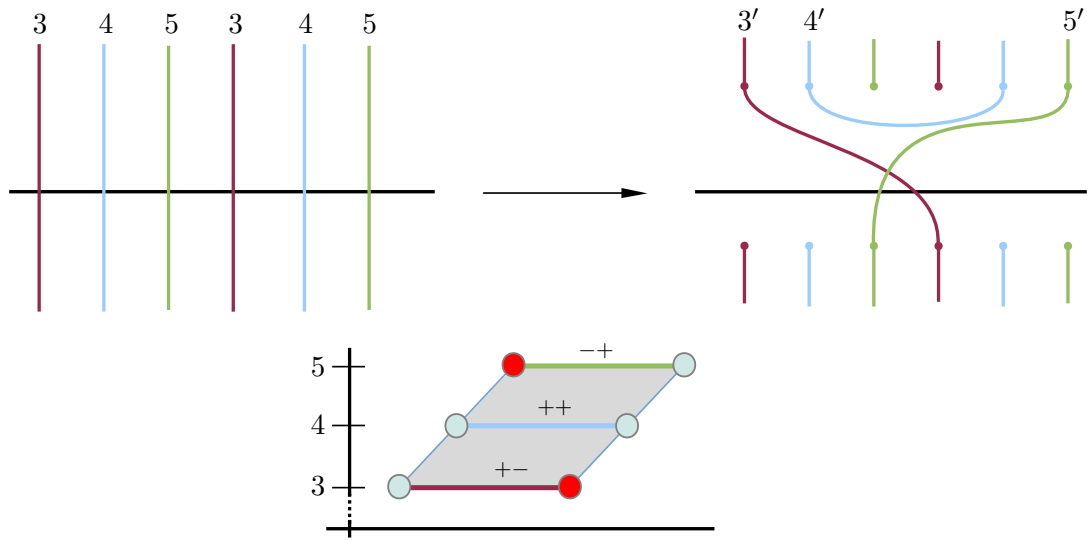


FIGURE 4. An example of a set of surgeries as in the box case.

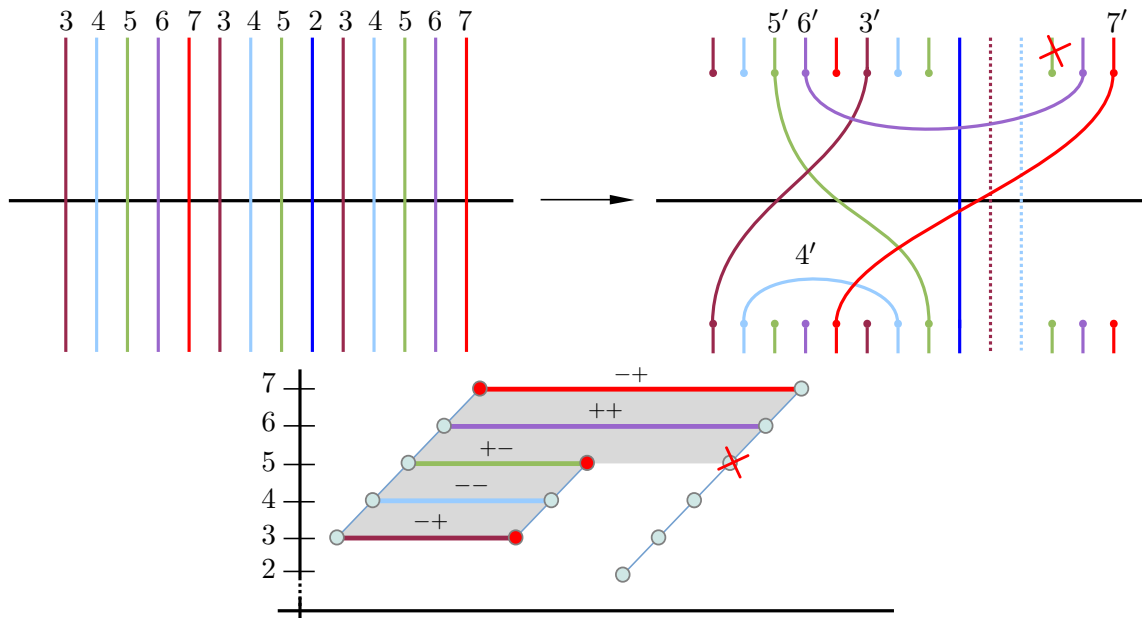


FIGURE 5. An example of a set of surgeries as in the hexagon case.

Given a path  $p$  with vertices  $v = v_0, v_1, \dots, v_d = w$  with  $d \geq 3$  in  $\mathcal{C}(S)$ , the *complexity* of the path  $p$  is defined to be

$$\kappa(p) = \sum_{k=1}^{d-1} (i(v_0, v_k) + i(v_k, v_d)).$$

Let  $p_1$  be the path  $v_d, v_{d-1}, v_{d-2}, v_{d-3}$  and  $p_k$  be the path  $v_{d-k-1}, v_{d-k-2}, \dots, v_d$  for  $2 \leq k \leq d-1$ . The *total complexity* of a path  $p$  is the lexicographically ordered (d-1)-tuple:

$$\hat{\kappa}(p) = (\kappa(p_1), \kappa(p_2), \dots, \kappa(p_{d-1})).$$

We will show that a geodesic of minimal complexity is initially super efficient. If  $d-1 \leq 15 \cdot (6g-8)$ , then the initial efficiency of the short geodesic is verified by the existence of initially efficient geodesics [4]. So we will mainly focus on the cases when  $d-1 > 15 \cdot (6g-8)$ . Suppose not, given a geodesic that is not initially super efficient, then either it is not of minimal complexity, or the geodesic has infinite length. The obstruction of a geodesic having minimal complexity is the occurrence of these three types of dot graph polygons. If such dot graph polygons occur, we can perform the corresponding curve surgeries to reduce the complexity. Here are some examples for the box surgery, Figure 4, and hexagon surgery, Figure 5. The outline of the proof is to guarantee that no such configuration in the dot graph eventually forces the geodesic have infinite length. The difficulty is to obtain an explicit bound of super initial efficiency that only depends on the genus of a surface. Ultimately, we will argue that the explicit bound can be taken to be  $15 \cdot (6g-8)$  for  $g \geq 3$  and 44 for  $g = 2$ .

#### 4. RAINBOW

Let  $v = v_0, v_1, \dots, v_d = w$  be a geodesic of minimal complexity with sufficiently large distance (i.e.,  $d > 15 \cdot (6g-8) + 1$  for  $g \geq 3$ , and  $d > 45$  for  $g = 2$ ), and  $\alpha_0, \alpha_1$  and  $\alpha_d$  are representatives intersecting minimally without any triple points. For any reference arc  $\gamma$  of the pair  $(\alpha_0, \alpha_d)$ , that is, an arc that is in minimal position with  $\alpha_1$  and whose interior is disjoint from  $\alpha_0 \cup \alpha_d$ . In fact, it suffices to look at the reference arc that connects the midpoints of  $\alpha_0$ -edges in a non-rectangular polygon of  $S_g \setminus (\alpha_0 \cup \alpha_d)$ .

We will show that if the intersection  $\alpha_1 \cap \gamma$  is sufficiently large, then it will create some parallel arcs of  $\alpha_1 \setminus \gamma$ , which in turn gives rise to parallel arcs of  $\alpha_i \setminus \gamma$  for some other curve  $\alpha_i$ . Our goal is to obtain such estimate of the intersection number to make this happen. This is a first step in our argument to show the process is infinite once we modify the estimate of the intersection number with reference arcs.

We start off with a calculation of one-vertex triangulation of a closed surface.

**Lemma 4.1.** *The number of edges in one-vertex triangulation of a closed oriented surface  $S_g$  is  $6g - 3$ .*

*Proof.* Consider a one-vertex triangulation of  $S_g$  with number of vertices, edges and faces denoted by  $V$ ,  $E$  and  $F$ , respectively. By Euler characteristic calculation,  $V - E + F = 2 - 2g$ . In the triangulation, each face has 3 edges and each edge is shared by 2 faces, then we have  $2E = 3F$ . Since there is a unique vertex, if we multiply the Euler characteristic by 3, then

$$(5) \quad \begin{aligned} 3V - 3E + 3F &= 6 - 6g, \\ 3V - 3E + 2E &= 6 - 6g, \\ 3V - E &= 6 - 6g, \\ 3 - E &= 6 - 6g, \\ E &= 6g - 3 = 3(2g - 1). \end{aligned}$$

□

Now focus on the components of  $\alpha_1 \setminus \gamma \subset S_g \setminus \alpha_0$ . Two arc components  $c_1, c_2 \subset \alpha_1 \setminus \gamma$  are *parallel* in  $S_g \setminus \alpha_0$  if they are two opposite sides of a rectangular disc—the other two sides being in  $\gamma$ . (See Figure 6.)

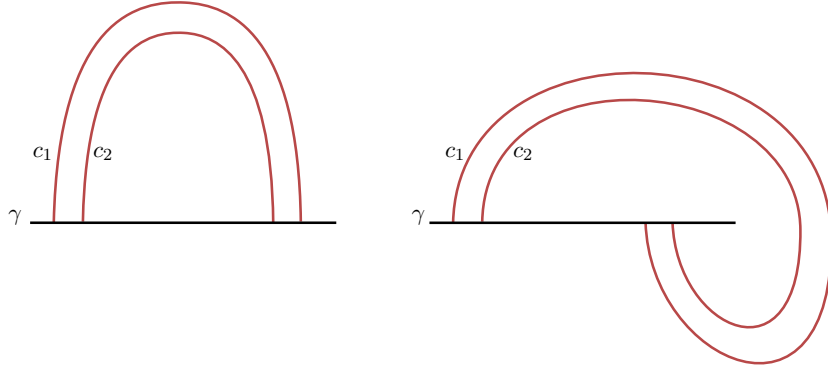


FIGURE 6. Two configurations of parallel arcs.

We want to decide the classes of parallel components of  $\alpha_1$ . When we split  $S_g$  along  $\alpha_0$ , the reference arc  $\gamma$  is a properly embedded arc with its endpoints on the boundary of the resulting surface,  $S_{\hat{g}}$ , where  $\hat{g} \leq g - 1$ .

There are three cases:

- (1)  $\alpha_0$  is non-separating and two endpoints of  $\gamma$  are on two distinct boundary components of the connected surface  $S_g \setminus \alpha_0$ ;
- (2)  $\alpha_0$  is non-separating and both endpoints of  $\gamma$  are on the same boundary component of the connected surface  $S_g \setminus \alpha_0$ ;

- (3)  $\alpha_0$  is separating and two endpoints of  $\gamma$  is on the single boundary component of one of the two components in  $S_g \setminus \alpha_0$ .

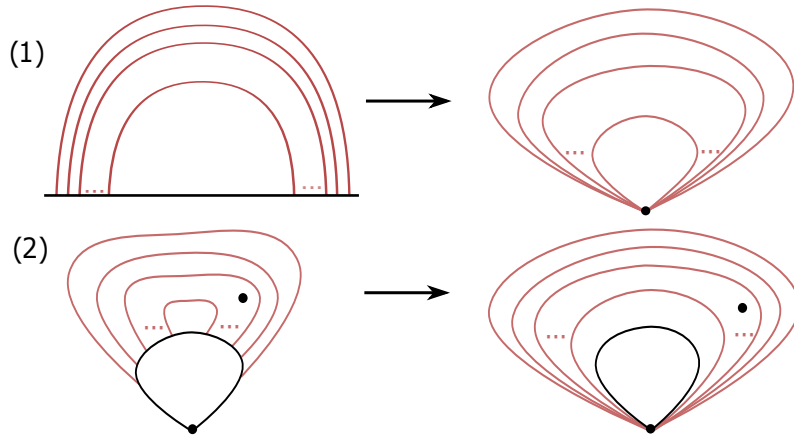


FIGURE 7. In (1), the reference arc  $\gamma$  in black with two endpoints on two distinct boundary components (two distinct vertices after being crushed) of  $S_g \setminus \alpha_0$  is collapsed to a point; In (2), two boundary components of  $S_g \setminus \alpha_0$  are crushed to two points. The two endpoints of the reference arc  $\gamma$  in black are identified to be a single endpoint, and the intersection points with  $\alpha_1$  are moved along  $\gamma$  to the single endpoint.

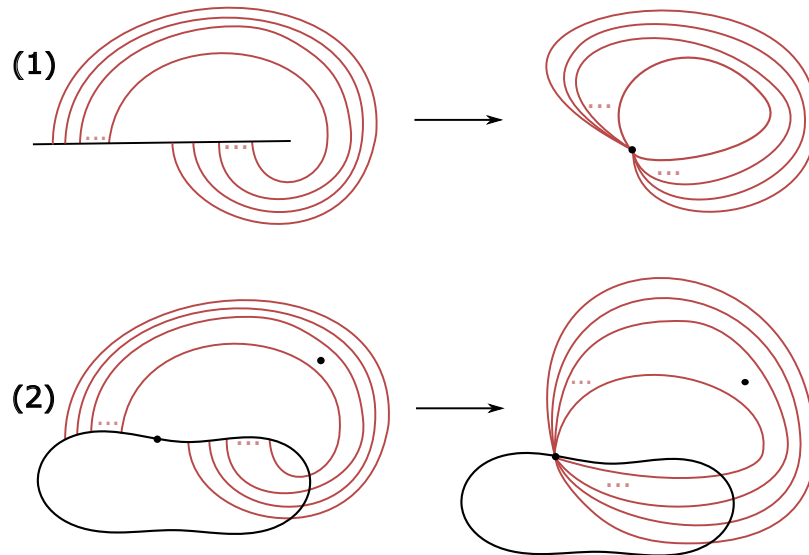


FIGURE 8. The other configuration is similar to Figure 7.

In all cases we can think of  $\gamma$  as being in a surface of at least one less genus with either one or two vertices (the boundary curves crushed to points). The Figures 7 & 8 are illustrated for the two configurations in the Figure 6. The two configurations are almost the same, so we only consider the left configuration.

In Figure 7(1), the two endpoints of the arc  $\gamma$  are on two distinct boundary components of  $S_g \setminus \alpha_0$ . The two boundary components are crushed to two points, and the arc  $\gamma$  is collapsed to a single point as well. It follows that the classes of parallel components of  $\alpha_1 \setminus \gamma$  is same as the number of edges in one-vertex triangulation of surface  $S_{g-1}$ . By Lemma 5, it is  $C_{\sharp} = 3(2(g-1) - 1) = 6g - 9$ .

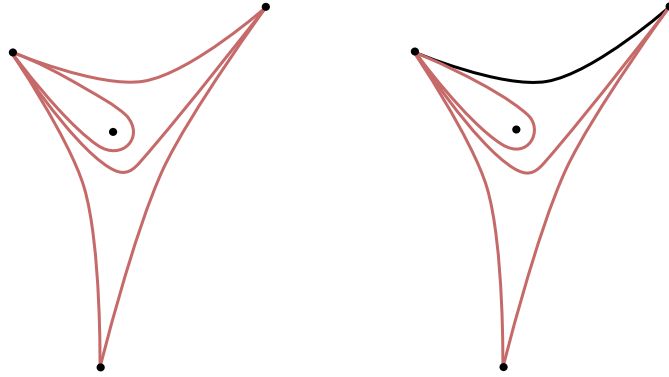


FIGURE 9. The triangles with one puncture are taken from the triangulation in the bottom right illustrations of Figures 7 and 8, in which the vertices of the triangles are identified to be one vertex. At most two more edges (two classes of parallel components of  $\alpha_1 \setminus \gamma$ ) can be added to the triangle.

In the second case, Figure 7(2), both endpoints of  $\gamma$  are on the same boundary/vertex of  $S_{\hat{g}}$ . The reference arc  $\gamma$  will be one of the edges of a one-vertex triangulation of a once punctured  $S_{g-1}$ . Since two more non-parallel edges can be added to the triangle containing the vertex crushed by the other boundary as illustrated in Figure 9. The components of  $\alpha_1 \setminus \gamma$  can have at most  $C_{\sharp}$ -classes of parallel components, where  $C_{\sharp} = 3(2(g-1) - 1) - 1 + 2 = 3(2(g-1) - 1) + 1 = 6g - 8$ .

In the third case, note that the number of classes of parallel components of  $\alpha_1$  would not be larger than that in the second case. Hence, in all cases, the most possible number of parallel components of  $\alpha_1 \setminus \gamma$  is  $C_{\sharp} = 3(2(g-1) - 1) + 1 = 6g - 8$ .

If  $\frac{n}{C_{\sharp}} > 1$ , then there must be at least two arcs of  $\alpha_1 \setminus \gamma$  that are parallel. More generally, if  $\frac{n}{C_{\sharp}} > k - 1$ , then by the pigeon hole principle, there must be at least  $k$  parallel arcs.

**Lemma 4.2** (Descending sawtooth forms). *The  $k$  parallel arcs of  $\alpha_1$  determines  $k$  ascending segments such that each ascending segment is one level less than its predecessor, that is, they form a descending sawtooth form.*

*Proof.* First, notice that by efficiency every rectangular disc illustrating the parallel nature of two arcs of  $\alpha_1 \setminus \gamma$  must contain/trap an arc of  $\alpha_2 \setminus \gamma$ . Otherwise, two parallel arcs allows a box surgery, so the complexity is not minimal. So consider two such rectangular discs stack together. That is, we have three parallel arcs,  $a_1^1, a_1^2, a_1^3 \subset \alpha_1 \setminus \gamma$  arranged with  $a_1^2$  being common to two rectangular discs. Then by efficiency there are arcs  $a_2^1, a_2^2 \subset \alpha_2 \setminus \gamma$  such that  $a_2^1$  is contained in the rectangular disc having  $a_1^1$  &  $a_1^2$  on its boundary; and,  $a_2^2$  is contained in the rectangular disc having  $a_1^2$  &  $a_1^3$  on its boundary. But, then this configuration will have  $a_2^1$  and  $a_2^2$  being parallel. Moreover, by efficiency again we must have an arc of  $\alpha_3 \setminus \gamma$  contained in the rectangular disc (which is a sub-disc of the two stack rectangular discs we started with) that illustrates  $a_2^1$  and  $a_2^2$  are parallel. (To drive the nail home, without an arc of  $\alpha_3 \setminus \gamma$  we would have a box surgery.) Figure 10 illustrates this stacking of two rectangular disc configuration. Similarly, the  $k$  parallel arc of  $\alpha_1$  traps  $k - 1$  arcs of  $\alpha_2$ , and that turns out to trap  $k - 2$  arcs of  $\alpha_3$ , etc.. In terms of dot graph, that means the  $k$  ascending segments are descending such that each of them is one level less than its predecessor. Although the  $k$  ascending segments are descending, there might exist some short ascending segments in between that would not violate the sawtooth condition.

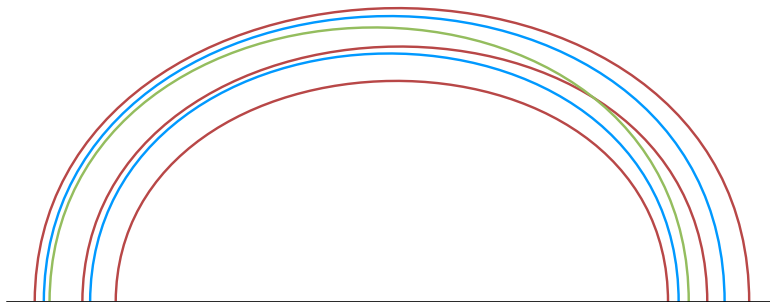


FIGURE 10. The three parallel arcs of  $\alpha_1$  are colored red; the two parallel arcs of  $\alpha_2$  are colored blue; and, the arc of  $\alpha_3$  is colored green.

□

The descending sawtooth form in a dot graph in the previous proposition forms a *rainbow* if we lay out all the parallel arcs. If we continue to play this stacking of

rectangular game we can force arcs of  $\alpha_i$ , with  $i$  increasing into a rainbow of parallel arcs. Figure 11 illustrates the configuration when we have five arcs of  $\alpha_1$  parallel. By efficiency, the stacking of five  $\alpha_1$  arcs forces the occurrence of four  $\alpha_2$  arcs between the  $\alpha_1$ 's; three  $\alpha_3$  arcs between the  $\alpha_2$ 's; and, two  $\alpha_4$  arcs between the  $\alpha_3$ 's. The illustration is actually missing a single arc between the two  $\alpha_4$  arcs (making a box surgery available) since the illustration is becoming cluttered, but efficiency requires that one should be inserted.

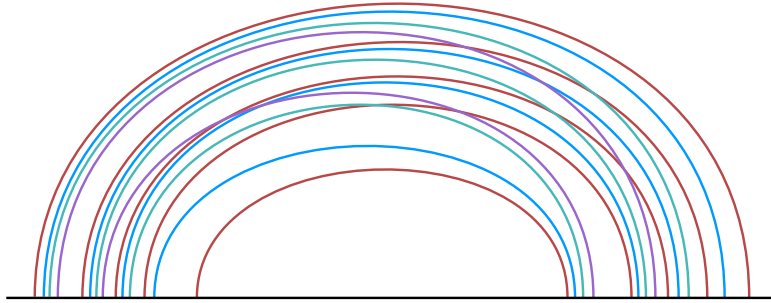


FIGURE 11. A 5-stack rainbow. Again parallel arcs of  $\alpha_1$  are colored red; arcs of  $\alpha_2$  are colored blue; arcs of  $\alpha_3$  is colored green; and, the single arc of  $\alpha_4$  is colored magenta.

Our argument in a nutshell is that,  $k$  parallel arcs of  $\alpha_1$  will force the existence of  $k$  parallel arcs of  $\alpha_{i_1}$ , for some  $i_1 > 1$ , which will force the existence of  $k$  parallel arcs of  $\alpha_{i_2}$ , for some  $i_2 > i_1$ , and etc.. Since all parallel arcs for each  $\alpha_{i_j}$  will have their endpoints on  $\gamma$  and since  $k$  is fixed, we get a contradiction in that our geodesic is of finite length but we have an infinite sequence of subarcs of  $\cdots, \alpha_{i_j}, \cdots, \alpha_{i_2}, \alpha_{i_1}, \alpha_1$ . The core of this argument is calculating a value for  $k$ . We start off with a warm-up case.

**Proposition 4.3.** *Let  $v = v_0, v_1, \cdots, v_d = w$  be a sufficiently long geodesic of minimal complexity in  $\mathcal{C}(S_{g \geq 2})$ ,  $\alpha_0, \alpha_1$  and  $\alpha_d$  be representatives of  $v_0, v_1$  and  $v_d$ , respectively. There exists an integer  $k$  satisfying that, for any reference arc  $\gamma$  of the pair  $(\alpha_0, \alpha_d)$  such that  $\alpha_1$  has  $k$  parallel arcs, then  $|a_{k+1} \cap \gamma| \geq k$ , where  $\alpha_{k+1}$  is a representative of  $v_{k+1}$ . More precisely,  $k = 5$  for  $g = 2$ ,  $k = 7$  for  $g = 3, 4, 5, 6, 7$ , and  $k = 8$  for  $g \geq 8$ .*

*Proof.* By Lemma 4.2, if we have a  $k$ -stack rainbow illustrating  $k$  parallel  $\alpha_1$  arcs then by efficiency the rainbow will contain an arc of  $\alpha_k$ . This point is key since the disjointness of  $\alpha_k$  and  $\alpha_{k+1}$  implies that  $\alpha_{k+1}$  cannot transversely intersect the rainbow. We now perform the obvious surgery that takes a union of an arc in the



rainbow of  $\alpha_1 \setminus \gamma$  and a subarc of  $\gamma$  to form loops that intersect  $\gamma$  either zero (for left configuration of Figure 6) or once (for right configuration of Figure 6). See Figure 12. Call this new loop  $\alpha'_1$  and notice that it does not intersect  $\alpha_0$ .

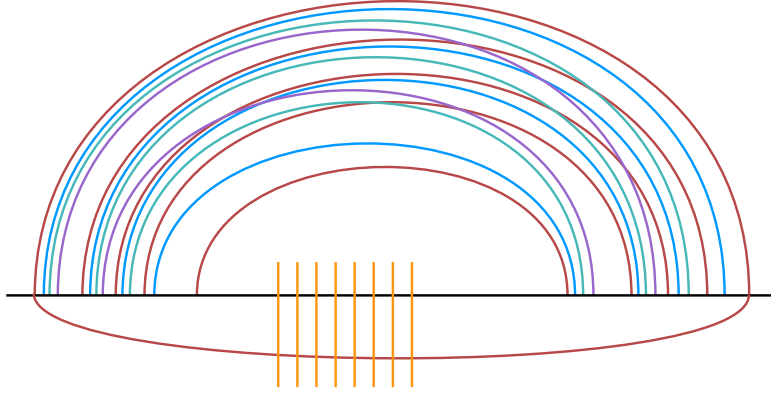


FIGURE 12. The  $\alpha'_1$  is the union of an outermost arc of  $\alpha_1$  and a subarc of  $\gamma$ .

Now consider  $|\alpha'_1 \cap \alpha_{k+1}|$ . Notice that since  $\alpha_{k+1}$  cannot intersect transversely the  $k$ -stack rainbow, the only place  $\alpha'_1$  can intersect  $\alpha_{k+1}$  is between the two “ends” of the rainbow as illustrated in Figure 12. Thus, each intersection of  $\alpha_{k+1}$  with  $\alpha'_1$  also corresponds to an intersection of  $\alpha_{k+1}$  with  $\gamma$ . Our strategy is to “drive up” the value of  $\alpha_{k+1} \cap \gamma$  so that there are at least  $k$  parallel arcs of  $\alpha_{k+1} \setminus \gamma$ . If so, we might repeat the above rainbow construction for these parallel  $\alpha_{k+1}$  arcs to say that we must have  $\alpha_{2k+1}$  intersecting  $\gamma$  enough times to have  $k$  parallel arcs. Then, an iteration of our rainbow construction never ends, a contradiction that the distance between  $\alpha_0$  and  $\alpha_d$  is finite.

With this in mind, we know that  $d(\alpha'_1, \alpha_{k+1}) \geq k$ , because  $|\alpha_0 \cap \alpha'_1| = 0$ . Now using Theorem 1.3 for  $g = 2$ , we have  $2^{k-4} \cdot 12 \leq |\alpha'_1 \cap \alpha_{k+1}| (= |\gamma \cap \alpha_{k+1}|)$  and  $C_{\sharp} = 6(2) - 8 = 4$ . To drive up this intersection number, we ask the question: for what value of  $k$  does

$$(6) \quad \frac{2^{k-4} \cdot 12}{C_{\sharp}} = \frac{2^{k-4} \cdot 12}{4} > k - 1?$$

Our initial answer is to have  $k = 5$ , and with  $|\alpha_1 \cap \gamma| > 4 \cdot 4 = 16$ , we will get a rainbow of  $\alpha_1$  arcs that is at least a 5-stack rainbow. We will need to come back to equation 6 later to increase the size of this  $\alpha_1$  rainbow for achieving a contradiction.

For  $g > 2$ , we have  $2^{k-3}(2g - 1) \leq |\alpha'_1 \cap \alpha_{k+1}| (= |\gamma \cap \alpha_{k+1}|)$ . To drive up this intersection number, our equation 6 is changed to asking for what value of  $k$  does

$$(7) \quad \frac{2^{k-3}(2g - 1)}{C_{\sharp}} = \frac{2^{k-3}(2g - 1)}{6g - 8} > k - 1?$$

When  $g = 3, 4, 5, 6, 7$ , then  $k = 7$  works. For  $g \geq 8$ ,  $k = 8$  always works. Again, to guarantee an 8-stack rainbow for arcs of  $\alpha_1$ ,  $|\alpha_1 \cap \gamma| > 7 \cdot (6g - 8)$ , we will need to come back to this calculation later to increase the size of the  $\alpha_1$  rainbow.  $\square$

With the same value  $k$  and condition as the above Proposition 4.3, we are able to generalize the result from  $\alpha_1$  to any curve.

**Proposition 4.4.** *If a curve  $\alpha_m$  has  $k$  parallel arcs with a reference arc  $\gamma$  for the pair  $(\alpha_0, \alpha_d)$ , then  $|a_{k+m} \cap \gamma| \geq k$ .*

## 5. PROOF OF SUPER EFFICIENCY

Our strategy now is to argue that when we iterate this construction, having a rainbow forces the existence of another rainbow with the stack number not decreasing, which makes our original geodesic of minimal complexity have infinite length, a contradiction.

More precisely, with Proposition 4.4, there are curves with higher indices trapped in the rainbow. On the other hand, it is possible that we can extend the curves trapped in the rainbow to the curves with lower indices. Once we fix the middle curve  $\alpha_{k+1}$ , we will search subarcs of  $\alpha_i$  with lowest index  $i$  and  $\alpha_j$  with highest index  $j$  trapped in the rainbow formed by the subarcs of  $\alpha_{k+1}$ . The process turns out to be a race between the distance between two curves  $\alpha_i$  and  $\alpha_{j+1}$  and the intersection number of  $\gamma \cap \alpha_{k+1}$ . We are looking for the worst scenario in which the distance on the left side is as small as possible while keeping the intersection number on the right side as larger as possible. In the next round,  $\alpha_{j+1}$  becomes the middle curve to form the rainbow, and the process continues forever, a contradiction.

But, there is a subtlety as we examine the rainbow at the next stage. Let us go to the general case that  $g > 2$ . For the  $g > 2$  case and having  $k = 8$ , our calculation gives us that  $\alpha'_1$  intersects  $\alpha_9$  at least  $2^{8-3} \cdot (2g - 1) = 32 \cdot (2g - 1)$  times; and, there must be at least  $11 (= \lceil \frac{32 \cdot (2g-1)}{6g-8} \rceil)$ -stack rainbow coming from parallel arcs of  $\alpha_9$ .

Let  $a_9^1, a_9^2, \dots, a_9^k \subset \gamma \cap \alpha_9$  be the listing of consecutive endpoints at one end of the  $k$  ( $k \geq 11$ )-stack rainbow formed by arcs of  $\alpha_9$ . Between  $a_9^i$  and  $a_9^{i+1}$  we must have either  $a_{10}$  or  $a_8$  intersect  $\gamma$  by efficiency of the geodesic. Otherwise, we can do a box surgery for the two consecutive intersection points, as illustrated in Figure 13.

*Proof of Theorem 1.1.* First, we argue that there must be an  $a_{10}$  between  $a_9^i$  and  $a_9^{i+1}$  for some  $1 \leq i \leq k - 1$ . Since there is no  $a_{10}$  intersecting the reference arc  $\gamma$  between  $a_9$ 's, to avoid the box surgery, there must be an  $a_8$  instead. By induction, there is an  $a_7$  on the  $a_8$ -level and so on. The upside down triangle in the right of Figure 14 illustrates this observation. As showed in Figure 14, since the first (previous) rainbow is at bottom left of the (current) rainbow, there is an ascending segment blocking the two horizontal edges as the intersection sequence is in sawtooth form.

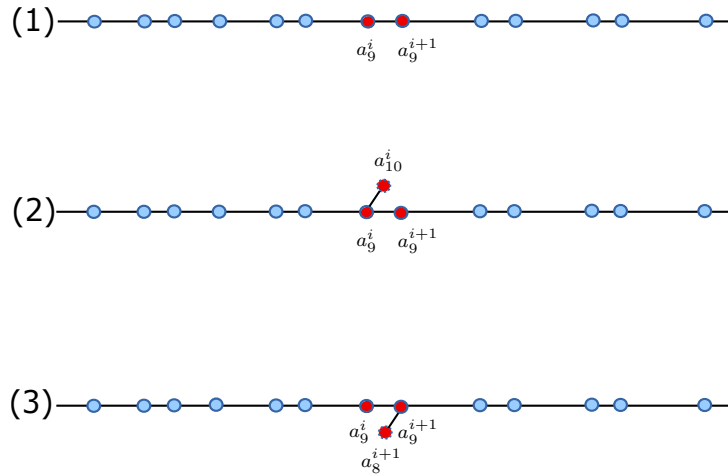


FIGURE 13. In (1), two adjacent intersection points  $a_9^i$  and  $a_9^{i+1}$  are in red; (2) and (3) illustrate two possible ways to insert  $\alpha_{10}$  or  $\alpha_8$  between two consecutive intersection points of  $\gamma \cap \alpha_9$  to avoid a box surgery.

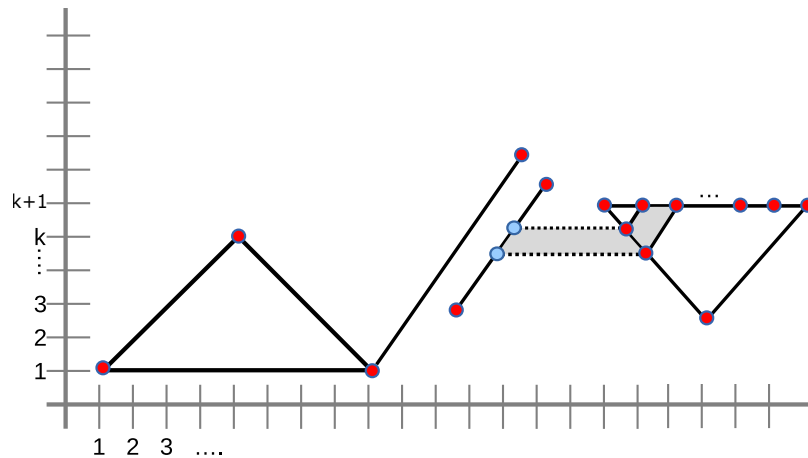


FIGURE 14. A hexagon surgery of type 2 occurs due to the (current) rainbow without any curve with higher index.

It follows that the two consecutive endpoints,  $a_9^i$  and  $a_9^{i+1}$ , creates a hexagon surgery of type 2.

More generally, there is an ascending segment starting with  $a_9$  between  $a_9^i$  and  $a_9^{i+1}$ . Suppose there is no  $a_8^{i+1}$  below  $a_9^{i+1}$ , then the next ascending segment must

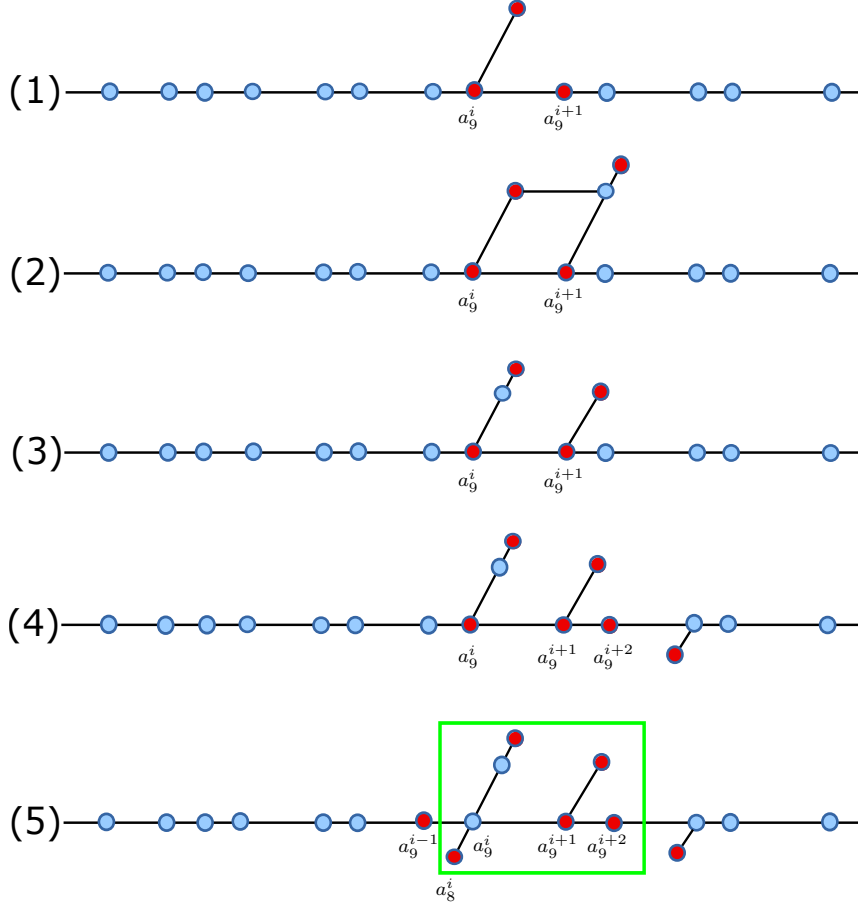


FIGURE 15. (1) Ascending segment starts with  $a_9^i$ ; (2) A box surgery occurs if the next ascending segment is not lower; (3) The highest index of the ascending segment is exactly one less; (4) Another  $a_9^{i+2}$  can be added; (5) Insert an  $a_8^i$  under  $a_9^i$ .

be lower to avoid a box surgery, see Figure 15. Recall that our goal is to reduce the distance, so the highest index should be exactly one less.

To put more intersection points of  $\gamma \cap \alpha_9$  on  $\gamma$ , we can insert a single  $a_9^{i+2}$  next to  $a_9^{i+1}$ . On the left side of  $a_9^i$ , we need to insert  $a_8^i$  to make  $a_9^{i-1}$  a single dot. Hence, if there is no smaller index of  $a_9^{i+1}$ , then the green box in Figure 15 contains a local optimal pattern.

On the other hand, if  $a_9^{i+1}$  does have  $a_8^{i+1}$ , then we can insert an additional  $a_9$  as illustrated in (2) of Figure 16. That means the additional  $a_9$  is  $a_9^{i+1}$  and the original  $a_9^{i+1}$  becomes  $a_9^{i+2}$ . The (3) and (4) in Figure 16 show that the next ascending segment should be lower, otherwise, a degenerate hexagon surgery occurs.

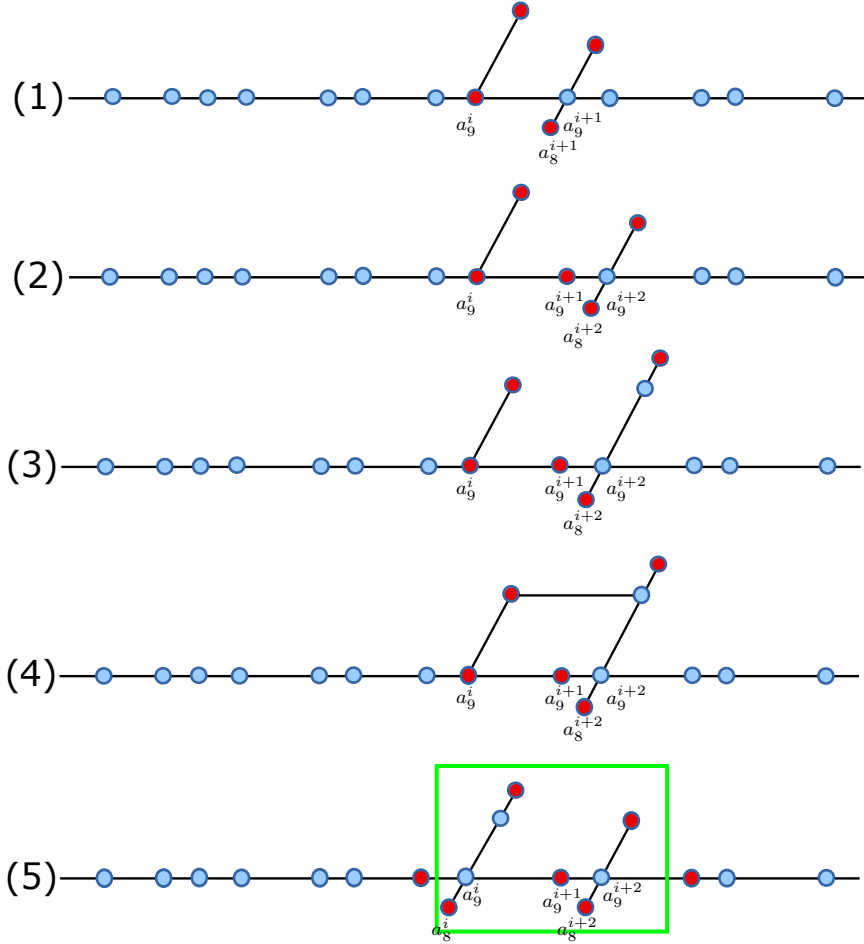


FIGURE 16. (1) An  $a_8^{i+1}$  under  $a_9^{i+1}$ ; (2) Another  $a_9$  can be inserted; (3) Next ascending segment is not lower; (4) A hexagon surgery; (5) The highest index of the ascending segment is exactly one less than that of the previous segment.

To reduce the indices slowly, the highest index of the ascending segment should be one less. The green box in Figure 16 contains another local optimal pattern.

Both local optimal patterns have three  $a_9$ 's, one of which is a single dot, and the other two are in two ascending segments. The highest index of the right is exactly one less than that of the left. The difference lies in the number of  $a_8$ 's. The first pattern only contains a single  $a_8$ , while the second one has two  $a_8$ 's.

To put it simple, if we iterate the two patterns independently, we will have the top illustrations in Figures 17 & 18. The violation of hexagon surgery forces the highest index of ascending segments is larger than that on the right. To make it to

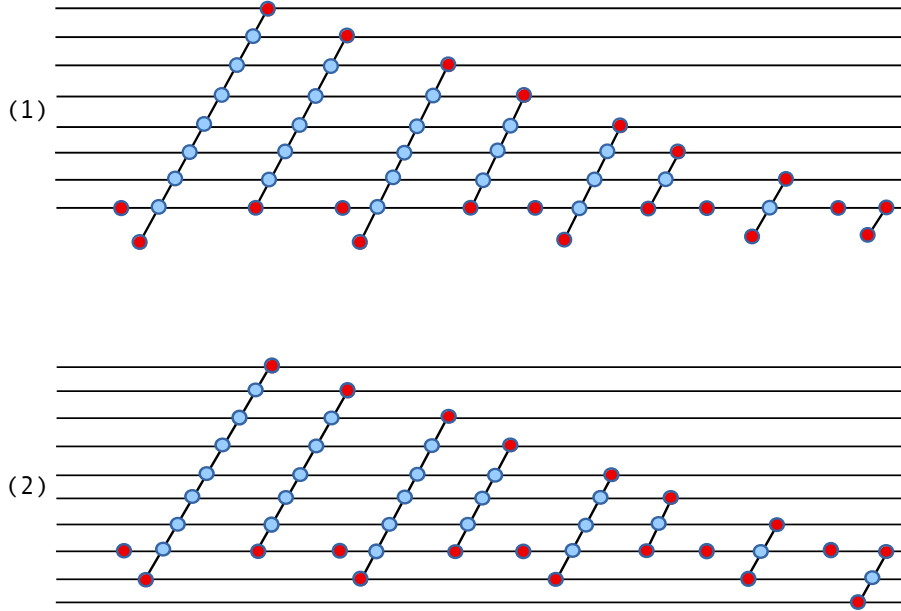


FIGURE 17. (1) Iteration of the first pattern; (2) Extend the dot graph below  $a_9$  level.

be optimal, highest indices decrease exactly one as we move along. If we extend the graph below  $a_9$ , we can observe a big difference between the two patterns.

In the first pattern, since there is only one  $a_8$  in each pattern, there is no need to add more  $a_8$  or  $a_7$  except for the rightmost ascending segment. It violates the efficiency if we don't put an  $a_7$ . The situation is quite different in the second pattern, as a hexagon surgery occurs in each pattern. To get rid of all these surgeries, we add the ascending segments as in Figure 18. In comparison to the previous pattern, it will significantly increase the distance, so it will not be the worst scenario. It follows that the worst case only consists of the first pattern. Generally, two patterns can be mixed, but each second pattern will add more curves. Hence, the worst scenario only contains the first pattern.

With this in mind, this allows us to define a function  $S(k)$  to be the difference of the highest index  $j$  and the lowest index  $i$  in Figure 17 type pattern having  $k$  dots at  $\alpha_9$  (middle curve). Similar to the first rainbow, we can construct a new curve by the subarc  $\alpha_i$  and  $\gamma$ , denoted as  $\alpha'_i$ . It follows that  $d(\alpha_{j+1}, \alpha'_i) \geq j - i - 1 = S(k) - 1$ , because  $d(\alpha'_i, \alpha_i) \leq 2$ . Each pattern has three dots, so we have three cases for the formula of  $S(k)$ .

In Figure 17, the intersection number  $k = 13$ , and we have  $S(13) = 9$ . When  $k = 12$ , we can remove the rightmost ascending segment, as shown in Figure 19. In

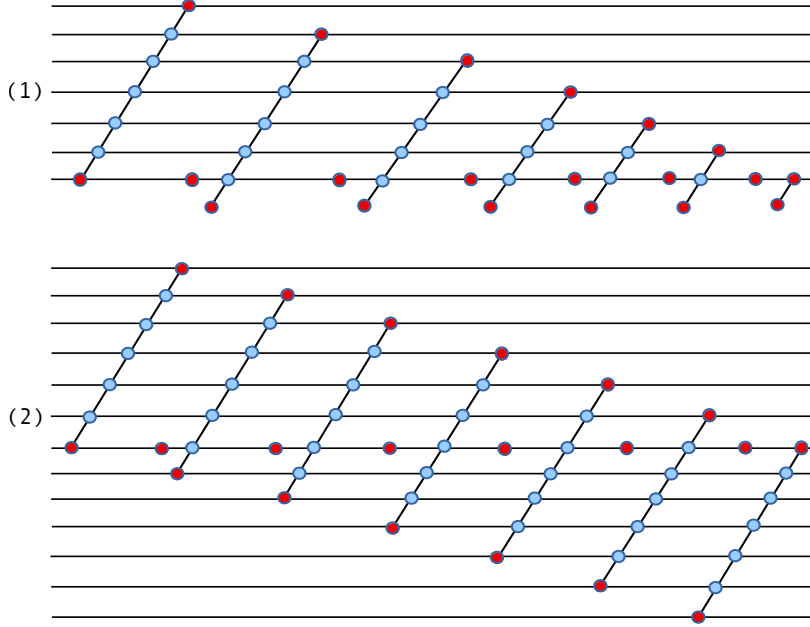


FIGURE 18. (1) Iteration of the second pattern; (2) Extend the dot graph below  $a_9$  level.

this case,  $S(12) = 8$ . When  $k = 14$ , either we can add a leftmost ascending segment, or add two leftmost ascending segment and remove the rightmost one. Figure 20 illustrates this case, but we have  $S(k) = 10$  for both cases.

More generally, the formula of  $S(k)$  is as follows.

$$(8) \quad S(k) = \begin{cases} 2p, & \text{if } k = 3p, \text{ for } p \geq 1 \\ 2p + 1, & \text{if } k = 3p + 1, \text{ for } p \geq 1 \\ 2p + 2, & \text{if } k = 3p + 2, \text{ for } p \geq 1 \end{cases}$$

Now we can repeat our previous calculation. For the case  $g > 2$ , so substituting  $3p$  for  $k$  on the right and  $S(k) - 1 = 2p - 1$  for  $k$  on the left in equation 7, we get:

$$(9) \quad \frac{2^{(2p-1)-3} \cdot (2g - 1)}{6g - 8} > 3p - 1.$$

In the case of  $g \geq 3$ , the solution is  $p \geq 5$ , so  $k = 15$ .

For the other two cases, let us first deal with  $k = 3p + 1$ , then

$$(10) \quad \frac{2^{((2p+1)-1)-3} \cdot (2g - 1)}{6g - 8} > (3p + 1) - 1.$$

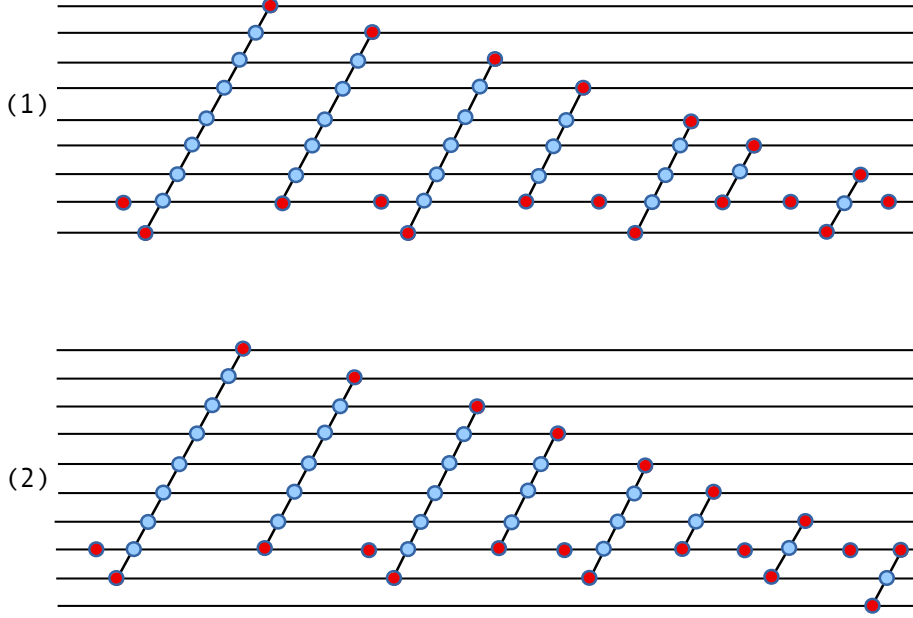


FIGURE 19. (1) The case when  $k = 12$ ,  $S(12) = 8$ ; (2) The case when  $k = 13$ ,  $S(13) = 9$ .

When  $g = 3, 4, 5, 6, 7$ , the solution is  $p \geq 4$ , so  $k = 13$ . It is  $p \geq 5$  for  $g \geq 8$ , so  $k = 16$ .

The other case is  $k = 3p + 2$ , and we have

$$(11) \quad \frac{2^{((2p+2)-1)-3} \cdot (2g-1)}{6g-8} > (3p+2) - 1.$$

The solution is  $p \geq 4$ , so  $k = 14$  for  $g \geq 3$ .

Now returning to our previous equation 7 calculation, we need to raise the value of  $k$  from 8 to  $k = 16$  for  $g \geq 3$ . To do this we need  $|\alpha_1 \cap \gamma| > 15 \cdot (6g - 8)$ .

For genus 2, our equations to solve are

$$(12) \quad \frac{2^{(2p-1)-4} \cdot (12)}{4} > 3p - 1.$$

$$(13) \quad \frac{2^{((2p+1)-1)-4} \cdot (12)}{4} > (3p+1) - 1.$$

$$(14) \quad \frac{2^{((2p+2)-1)-4} \cdot (12)}{4} > (3p+2) - 1.$$



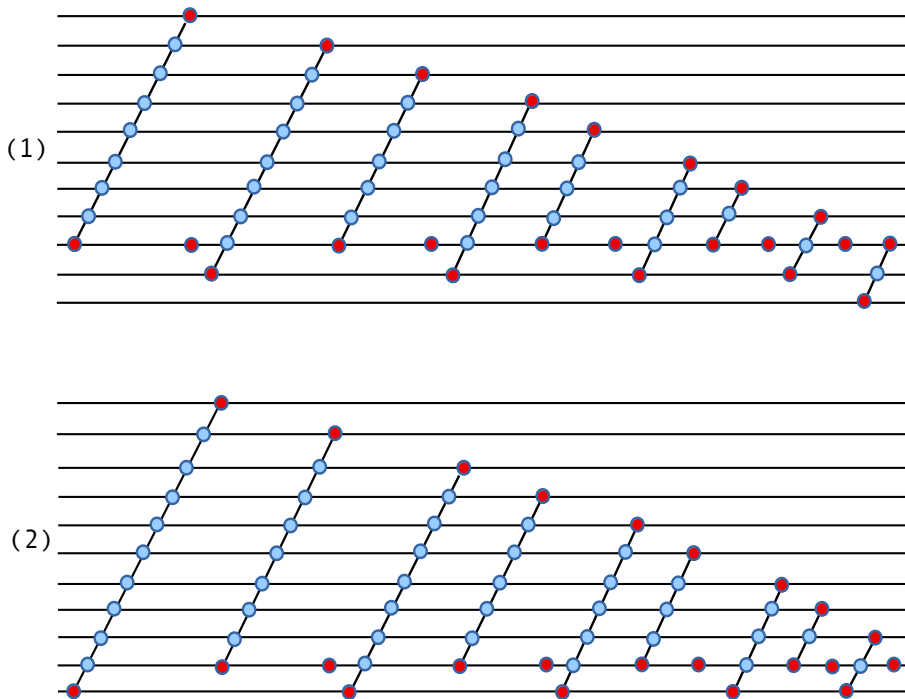


FIGURE 20. (1) and (2) are two cases when  $k = 14$ ,  $S(14) = 10$ .

For the three cases, the solutions are  $p \geq 4$ ,  $p \geq 3$  and  $p \geq 3$ , then  $k = 12$ ,  $k = 10$  and  $k = 11$ , respectively.

Now returning back to our previous equation 6 calculation, we need to raise the value of  $k$  from 5 to  $k = 12$ . To do this we need  $|\alpha_1 \cap \gamma| > 11 \cdot (4) = 44$ , for  $g = 2$ . Then we have our result that the geodesic of minimal complexity is initially super efficient with the stated bound. Now, we take the geodesics with minimal total complexity, the existence of super efficient geodesics follows immediately as Theorem 1.1 in [4].

□

**Remark 5.1.** For genus  $g \geq 7$ , it is not possible to improve the bounds of Theorem 1.1 by carrying out the previous calculation with Bowditch's growth estimate in Remark 1.6 that is equivalent to the inequality,

$$(\sqrt{2})^d \cdot (g - 2) < |\alpha \cap \beta|.$$

This observation can be illustrated by the following Figure 21.

Once we have Theorem 1.1, the proof of Corollary 1.2 is analogous to that of Theorem 1.1 in [4].

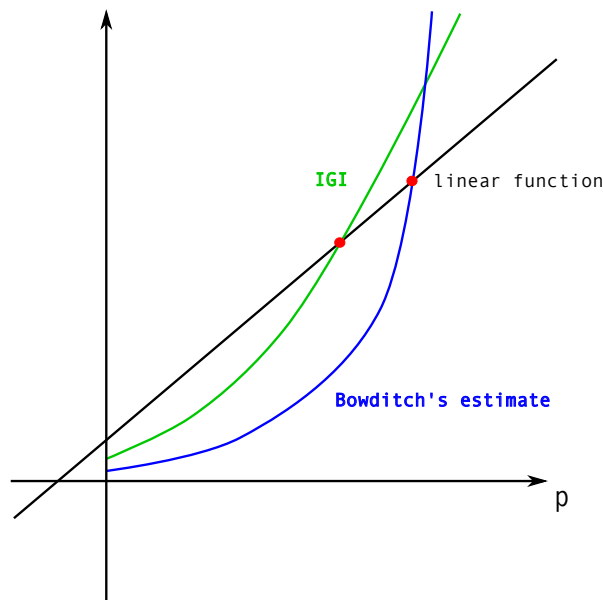


FIGURE 21. The relation among these three functions when the genus  $g \geq 7$ .

*Proof of Corollary 1.2.* Let  $\alpha_0, \alpha_1$  and  $\alpha_n$  be representatives of  $v_0, v_1$  and  $v_n$  with pairwise minimal intersection. For the polygons in  $S_g \setminus \alpha_0$  that are non-hexagons, we can cut through them along some reference arcs to make them to be hexagons. With this in mind, we end up with polygons as rectangles and hexagons. By Euler characteristic calculation, there are  $4g - 4$  hexagons. Since the reference arcs in rectangles are parallel to the adjacent ones in the hexagons, then they will be only counted once, so there are  $6g - 6$  reference arcs in total. Up to homotopy, the intersection number of  $\alpha_1$  with each reference arc determines  $\alpha_1$ . By Theorem 1.1, the choice of intersection number is at most  $15 \cdot (6g - 8) + 1$  for each reference arc, so there are at most  $[15 \cdot (6g - 8) + 1]^{6g-6}$  candidates for  $v_1$ . For  $g = 2$ , it is  $45^6$ .  $\square$

#### REFERENCES

- [1] Tarik Aougab. *Uniform hyperbolicity of the graphs of curves*. *Geom. Topol.*, 17 (2013), no. 5, 2855 - 2875.
- [2] Tarik Aougab, Priyam Patel, Samuel J. Taylor. *Covers of surfaces, Kleinian groups, and the curve complex*. <https://arxiv.org/abs/1810.12953>

- [3] Mark C. Bell and Richard C. H. Webb. *Polynomial-time algorithms for the curve graph*. <https://arxiv.org/abs/1609.09392>
- [4] Joan Birman, Dan Margalit, and William Menasco. *Efficient geodesics and an effective algorithm for distance in the complex of curves*. *Math. Ann.*, 366:1253–1279, 2016.
- [5] Brian H. Bowditch. *Uniform hyperbolicity of the curve graphs*. *Pacific J. Math.*, 269(2):269–280, 2014.
- [6] Paul Glenn, William W. Menasco, Kayla Morrell, and Matthew Morse. *Metric In The Curve Complex*. software, available at [micc.github.io](https://github.com/micc), 2014.
- [7] Paul Glenn, William W. Menasco, Kayla Morrell, and Matthew Morse. *MICC: A Tool For Computing Short Distances In The Curve Complex*. *Journal of Symbolic Computation*, Special issue on Algorithms and Software for Computational Topology:115–132, 2017.
- [8] William J. Harvey. *Boundary structure of the modular group*. pages 245–251, 1981. in: Riemann surfaces and related topics. Proceedings of the 1978 Stony Brook Conference (Stony Brook 1978), *Ann. of Math. Stud.* 97,.
- [9] John Hempel. *3-manifolds as viewed from the curve complex*. *Topology*, 40:631–657, 2001.
- [10] Jason Paige Leasure. *Geodesics in the complex of curves of a surface*. ProQuest LLC, Ann Arbor, MI, 2002. Thesis (Ph.D.)—The University of Texas at Austin.
- [11] Howard A. Masur and Yair N. Minsky. *Geometry of the complex of curves. I. Hyperbolicity*. *Invent. Math.*, 138(1):103–149, 1999.
- [12] Howard A. Masur and Yair N. Minsky. *Geometry of the complex of curves II: Hierarchical Structure*. *Geom. Funct. Anal.* 10 (2000), no. 4, 902 - 974.
- [13] Kenneth J. Shackleton. *Tightness and computing distances in the curve complex*. *Geom. Dedicata*, 160:243–259, 2012.
- [14] Yohsuke Watanabe. *Intersection numbers in the curve graph with a uniform constant*. *Topology Appl.*, 204:157–167, 2016.
- [15] Richard C. H. Webb. *Combinatorics of tight geodesics and stable lengths*. *Trans. Amer. Math. Soc.*, 367(10):7323–7342, 2015.

XIFENG JIN, DEPARTMENT OF MATHEMATICS, UNIVERSITY AT BUFFALO—SUNY, BUFFALO, NY 14260-2900, USA, XIFENGJI@BUFFALO.EDU

WILLIAM W. MENASCO, DEPARTMENT OF MATHEMATICS, UNIVERSITY AT BUFFALO—SUNY, BUFFALO, NY 14260-2900, USA, MENASCO@BUFFALO.EDU